# Mechanism of the Chemoselective and Stereoselective Ring Opening of Oxathiaphospholanes: An Ab Initio Study

Tadafumi Uchimaru,*,† Wojciech J. Stec,‡ and Kazunari Taira§

*Department of Physical Chemistry, National Institute of Materials and Chemical Research, Agency of Industrial Science and Technology, MITI, Tsukuba Science City 305, Japan, Institute of Applied Biochemistry, Tsukuba University, Tsukuba Science City 305, Japan, and Department of Bioorganic Chemistry, Centre of Molecular and Macromolecular Studies, The Polish Academy of Sciences, 90-363 Lodz, Sienkiewicza 112, Poland*

*Received November 26, 1996 (Revised Manuscript Received May 15, 1997⊗ )*

Ab initio investigations of the reaction profiles for the base-catalyzed methanolysis of amino-2-thiono-1,3,2-oxathiaphospholane suggested that ring opening with a retention of configuration at phosphorus would be energetically favorable, which provides a reasonable interpretation for the chemo- and stereoselectivity that have been determined experimentally for the reaction of diastereomerically pure 2-[(1-(α-naphthyl)ethyl)amino]-2-thiono-1,3,2-oxathiaphospholane. Nucleophilic attack at phosphorus will lead to a trigonal bipyramidal (TBP) pentacoordinate phosphorane intermediate, and pseudorotation will then occur concomitantly with collapse of the TBP intermediate. Thus, pseudorotation is strongly coupled with the reaction coordinate for the substitution pathway. This finding suggests that substitution with a retention of configuration can occur even though a TBP species resulting from pseudorotation fails to exist as an intermediate.

## Introduction

The stereocontrolled synthesis of nucleic acids with phosphorothioate linkages has recently received considerable interest. 5′-*O*-Dimethoxytrityl-nucleoside 3′-*O*-(2-thiono-1,3,2-oxathiaphospholane) gives dinucleoside 3′,5′-phosphorothioate upon treatment with 5′-OH nucleoside under base-catalyzed conditions.[1−3] This reaction makes it possible to synthesize diastereomerically pure nucleoside with a 3′,5′-phosphorothioate linkage. However, the stereochemical outcome of the ring opening of five-membered 1,3,2-oxathiaphospholane was unclear, and the absolute configuration at phosphorus was unable to be assigned.

A recent X-ray crystallography analysis by Uznanski *et al.*[2] has revealed that the DBU-catalyzed ring opening of diastereomerically pure 2-[(1-(α-naphthyl)ethyl)amino]-2-thiono-1,3,2-oxathiaphospholane (**1a**) occurs with a retention of configuration at phosphorus (eq 1).[2] Base-catalyzed methanolysis of ($R_p$,$R_c$)-1,3,2-oxathiaphospholane **1a**, followed by S-methylation of the intermediate, gave ($S_p$,$R_c$)-*O*,*S*-dimethyl *N*-[1-(α-naphthyl)ethyl]phosphoramidothioate (**3a**) in a nearly quantitative yield. Thus, the precursor of ($S_p$,$R_c$)-**3a** should be anionic ($S_p$,$R_c$)-**2a**.

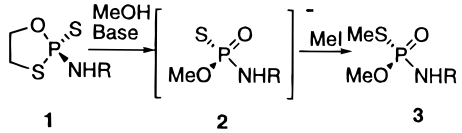


(1)

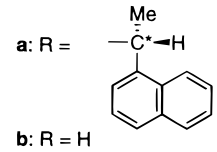


Westheimer's guidelines are commonly accepted for the mechanism of nucleophilic substitution at tetrahedral phosphorus.[4,5] Attack of a nucleophile will lead to a trigonal bipyramidal (TBP) pentacoordinate intermediate. Both the attacking and leaving groups will occupy axial positions in the TBP intermediate (axial entry and axial departure). The TBP intermediate is nonrigid and may undergo a rapid rearrangement of ligand positions via Berry pseudorotation.[6−8] This process involves concerted inward bond bending of both axial ligands and outward bending of two equatorial ligands (excluding that used as a pivot) to yield another TBP intermediate in which the axial and equatorial ligand pairs have exchanged positions. A square pyramidal transition state is postulated for pseudorotation. In addition, the diequatorial five-membered ring in a TBP phosphorane species is highly strained and quite unlikely.[5,9]

According to Westheimer's guidelines, pathways A−C in Scheme 1 are possible for the nucleophilic ring opening of 1,3,2-oxathiaphospholane.[2] Pseudorotation in the TBP intermediate is mandatory for a retention of configuration at phosphorus (Scheme 2).[4,5,10] Thus, only reaction pathway A, which involves axial entry, pseudorotation, and axial departure, resulting in the intermediate $I^{TH}_A$,

* To whom correspondence should be addressed. Tel: +81-298-54-4522. Fax: +81-298-54-4487. E-mail: t_uchimaru@nimc.go.jp.
† National Institute of Materials and Chemical Research.
‡ The Polish Academy of Sciences.
§ Tsukuba University.
⊗ Abstract published in *Advance ACS Abstracts,* August 1, 1997.

(1) Stec, W. J.; Grajkowski, A.; Koziolkiewicz, M.; Uznanski, B. *Nucleic Acids Res.* **1991**, *19*, 5883−5888.
(2) Uznanski, B.; Grajkowski, A.; Krzyzanowska, B.; Kazmierkowska, A.; Stec, W. J.; Wieczorek, M. W.; Blaszczyk, J. *J. Am. Chem. Soc.* **1992**, *114*, 10197−10202.
(3) Stec, W. J.; Grajkowski, A.; Kobylanska, A.; Karwowski, B.; Koziolkiewicz, M.; Misiura, K.; Okruszek, A.; Wilk, A.; Guga, P.; Boczkowska, M. *J. Am. Chem. Soc.* **1995**, *117*, 12019−12029.
(4) Westheimer, F. H. *Acc. Chem. Res.* **1968**, *1*, 70−78.
(5) Thatcher, G. R. J.; Kluger, R. *Adv. Phys. Org. Chem.* **1989**, *25*, 99−265.
(6) Berry, R. S. *J. Chem. Phys.* **1960**, *32*, 933−938.
(7) Mislow, K. *Acc. Chem. Res.* **1970**, *3*, 321−331.
(8) An alternative turnstile process has been proposed; see: Ugi, I.; Marquarding, D.; Klusacek, H.; Gillespie, P.; Ramirez, F. *Acc. Chem. Res.* **1971**, *4*, 288−296. Experimental results have generally been interpreted in terms of the Berry process: Russegger, P.; Brickmann, J. *Chem. Phys. Lett.* **1975**, *30*, 276−278.
(9) Holmes, R. R. *J. Am. Chem. Soc.* **1978**, *100*, 433−446.
(10) Deiters, J. A.; Holmes, R. R.; Holmes, J. M. *J. Am. Chem. Soc.* **1988**, *110*, 7672−7681.

S0022-3263(96)02220-7 CCC: $14.00 

**Scheme 1. Possible Pathways for the Base-Catalyzed Methanolysis of Oxathiaphospholane 1b[a]**

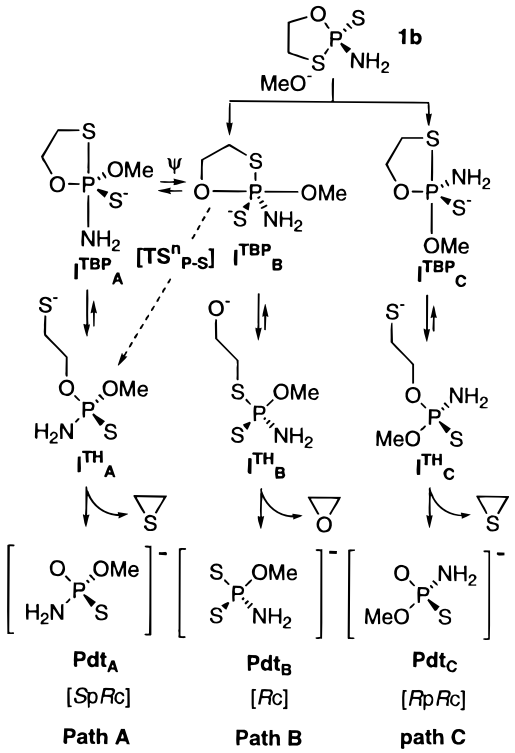


[a] ψ indicates a pseudorotation process.

**Scheme 2. Commonly Accepted Mechanism for Nucleophilic Substitution Reactions at Phosphorus[a]**

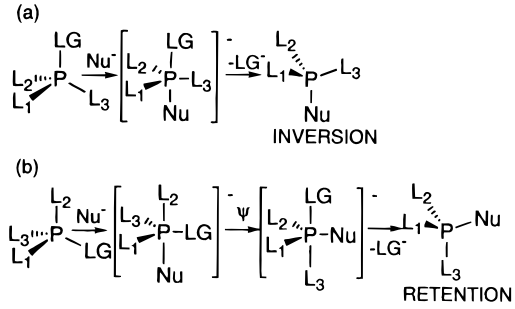


[a] (a) Axial entry and axial departure without pseudorotation (in-line mechanism) results in an inversion of the configuration at phosphorus. (b) Westheimer's guidelines suggest a mechanism which involves axial entry, pseudorotation, and axial departure for a retention of configuration at phosphorus resulting from nucleophilic displacement.

followed by elimination of thiirane, is consistent with the chemo- and stereoselectivity that have been determined experimentally for the ring opening of 1,3,2-oxathiaphospholane.[2,3] However, the TBP intermediate $I^{TBP}_A$ which results from pseudorotation would seem to be significantly unstable compared with the original TBP intermediate $I^{TBP}_B$: both sulfur and nitrogen ligands are less apicophilic than the oxygen ligand.[5,9,11−14] Indeed, Holmes' model for calculating conformational energies in pentacoordinate phosphorus compounds[5,9] suggests that $I^{TBP}_A$ should be 10.0 kcal/mol higher in energy than $I^{TBP}_B$.

The ab initio work of Lim and Tole in 1992 suggested a new mechanism for the base-catalyzed hydrolysis of methyl ethylene phosphate.[15,16] They found that the reaction coordinate of the attack of hydroxide anion at phosphorus is strongly coupled with pseudorotation in the gas phase. Contrary to Westheimer's guidelines, their observation suggests that concerted pseudorotation and formation/cleavage of an equatorial bond in TBP species is a viable mechanism for nucleophilic substitution with a retention of configuration at phosphorus. This observation was also extended to the hydrolysis of methyl aminoethylenephosphonate[17] and sulfate esters.[18]

By using a model system **1b** (eq 1), we examined ab initio reaction profiles with respect to pathways A−C (Scheme 1), as well as a pathway for concerted pseudorotation (indicated by the broken arrow in Scheme 1). The investigation described here extends the mechanism suggested by Lim and Tole to nucleophilic ring opening of 1,3,2-oxathiaphospholane and provides a reasonable interpretation for the chemo- and stereoselectivity that have been determined experimentally.[2,3] Thus, even though the TBP species resulting from pseudorotation fails to exist as an intermediate, substitution with a retention of configuration at phosphorus is still possible.

## Details of Computation

All calculations used the Gaussian 92 software package.[19] In some cases, the Gaussian 94 software package[20] and the Spartan software suite[21] were used. The split valence basis set with polarization and diffuse functions (6-31+G(D)) was used. We optimized all structures at the Hartree−Fock (HF) level and then evaluated the energies of each stationary point by MP2 (frozen core) single-point calculations. In specific instances, we performed geometry optimizations at the MP2 level and then evaluated MP4(DQ) energies (frozen core) at the MP2 geometries. Geometry optimizations used the standard convergence criteria in the software.[19,20] Frequency calculations (analytical method for HF and numerical method for MP2) were carried out for all stationary points to ensure adequate convergence. In addition, natural bond orbital (NBO) analyses[22−27] were carried out for several stationary points. We examined the energetic consequences of hyper-

(11) Hoffmann, R.; Howell, J. M.; Mutterties, E. L. *J. Am. Chem. Soc.* **1972**, *94*, 3047−3058.
(12) Strich, A.; Veliiard, A. *J. Am. Chem. Soc.* **1973**, *95*, 5574−5581.
(13) McDowell, R. S.; Streitwieser, A., Jr. *J. Am. Chem. Soc.* **1985**, *107*, 5849−5855.
(14) Wang, P.; Zhang, Y.; Glasser, R.; Reed, A. E.; Schleyer, P. v. R.; Streitwieser, A. *J. Am. Chem. Soc.* **1991**, *113*, 55−64.
(15) Lim, C.; Tole, P. *J. Phys. Chem.* **1992**, *96*, 5217−5219.
(16) Tole, P.; Lim, C. *J. Phys. Chem.* **1993**, *97*, 6212−6219.
(17) Tole, P.; Lim, C. *J. Am. Chem. Soc.* **1994**, *116*, 3922−3931.
(18) Cameron, D. R.; Thatcher, G. R. J. *J. Org. Chem.* **1996**, *61*, 5986−5997.
(19) Frisch, M. J.; Trucks, G. W.; Head-Gordon, M.; Gill, P. M. W.; Wong, M. W.; Foresman, J. B.; Johnson, B. G.; Schlegel, H. B.; Robb, M. A.; Replogle, E. S.; Gomperts, R.; Andres, J. L.; Raghavachari, K.; Binkley, J. S.; Gonzalez, C.; Martin, R. L.; Fox, D. J.; Defrees, D. J.; Baker, J.; Stewart, J. J. P.; Pople, J. A. Gaussian 92; Gaussian, Inc.: Pittsburgh, PA, 1992.
(20) Frisch, M. J.; Trucks, G. W.; Schlegel, H. B.; Gill, P. M. W.; Johnson, B. G.; Robb, M. A.; Cheeseman, J. R.; Keith, T. A.; Petersson, G. A.; Montgomery, J. A.; Raghavachari, K.; Al-Laham, M. A.; Zakrzewski, V. G.; Ortiz, J. V.; Foresman, J. B.; Cioslowski, J.; Stefanov, B. B.; Nanayakkara, A.; Challacombe, M.; Peng, C. Y.; Ayala, P. Y.; Chen, W.; Wong, M. W.; Andres, J. L.; Replogle, E. S.; Gomperts, R.; Martin, R. L.; Fox, D. J.; Binkley, J. S.; Defrees, D. J.; Baker, J.; Stewart, J. P.; Head-Gordon, M.; Gonzalez, C.; Pople, J. A. Gaussian 94; Gaussian, Inc.: Pittsburgh, PA, 1995.
(21) Carpenter, J. E.; Hehre, W. J.; Kahn, S. D. Spartan version 4.0; Wavefunction Inc.: Irvine, CA.
(22) Foster, J. P.; Weinhold, F. *J. Am. Chem. Soc.* **1980**, *102*, 7211−7218.
(23) Reed, A. E.; Weinhold, F. *J. Chem. Phys.* **1983**, *78*, 4066−4073.
(24) Reed, A. E.; Weinstock, R. B.; Weinhold, F. *J. Chem. Phys.* **1985**, *83*, 735−746.
(25) Carpenter, J. E.; Weinhold, F. *THEOCHEM* **1988**, *169*, 41−62.

conjugative delocalization by deleting the off-diagonal Fock matrix elements in the NBO basis.

A continuum dielectric model has been employed to evaluate the solvation effects on the hydrolysis of phosphates[16,17,28,29] and sulfates.[18] In a continuum dielectric model, a solute molecule is placed in a cavity immersed in a continuous medium with a dielectric constant $\epsilon$. The simplest model is the Onsager reaction field model. Despite its simplicity (a spherical cavity and considering just a dipole), the Onsager model has been found to be useful for qualitatively reproducing solution-phase behavior.[30−33] Interaction between the dipole in the solute molecule and the electric field due to the induced dipole in the medium will lead to net stabilization.

We used the Onsager model to estimate the solvation effects on the transition states, as well as on the most stable TBP intermediate. The ring opening of 1,3,2-oxathiaphospholane **1a** was observed in a pyridine/acetonitrile or benzene/acetonitrile solvent system.[1−3] The dielectric constant of acetonitrile ($\epsilon$ = 36.7) was used for these calculations. The cavity radii were calculated using the quantum mechanical method[34] for gas-phase structures. The geometries of the stationary points were optimized at the HF level by using the recommended values for the cavity radii, which were 0.5 Å larger than those computed for a contour of 0.001 electrons/bohr$^3$. Relative stabilities of the stationary points were evaluated at the HF geometries using the common cavity radius (4.6 Å).

**Nomenclature.** We identify structures in the following manner. I, Ts, and IL represent intermediates, transition states, and long-range ion−dipole minima, respectively. Pdt is a product resulting from elimination of a thiirane or oxirane molecule. Subscripts A, B, and C indicate possible reaction pathways (Scheme 1). Superscripts TBP and TH following I distinguish between trigonal bipyramidal and tetrahedral structures. Subscripts of t and g distinguish between conformational isomers with regard to the methoxyl group in the TBP intermediates (*trans* and *gauche* relative to the endocyclic sulfur atom). Superscripts n and x following TS represent transition states for cleavage/formation of endocyclic and exocyclic bonds, respectively, in the TBP intermediates. These transition states are also characterized by the subscripts P−O or P−S, indicating cleavage/formation of the P−O or P−S bond. The transition states for elimination of thiirane and oxirane molecules are identified by the superscripts elim-T and elim-O, respectively.

## Results

**Conformation of 1b and Its Anion.** Only one conformer was found for **1b**. The HF-optimized bond lengths and bond angles in the 1,3,2-oxathiaphospholane ring in **1b** were in good agreement with those for the X-ray crystallographic structure of **1a**.[35,36]

The anion of **1b** had two distinct conformers, in which the N−H bond is *cis* and *trans* relative to the exocyclic sulfur atom. The energy difference between these conformers is insignificant. Due to the negative charge on the nitrogen atom, the P−N bond is shorter than that in neutral **1b**. Conversely, the bonds between phosphorus and the other three ligands are lengthened.

**Long-Range Complexes of 1b/1b Anion and MeO$^-$/MeOH.** We were able to locate minima of the long-range ion−dipole complexes. While two energetically identical minima were found for the complex of **1b** anion and methanol [IL(**1b**$^-$ + MeOH)], the complex of **1b** and methoxide anion [IL(**1b** + MeO$^-$)] had only one minimum. In these ion−dipole complexes, methanol or methoxide anion was located opposite the exocyclic P−S bond. Among the four ligand atoms of phosphorus, the exocyclic nitrogen atom in **1b** or **1b**$^-$ was closest to the oxygen atom of methanol or methoxide anion. Since methanol is much smaller than **1b**, deprotonation of methanol results in significantly greater destabilization than deprotonation of **1b** in the gas phase. Thus, gas-phase calculations suggested that the ion−dipole complex IL(**1b** + MeO$^-$) was much higher in energy than IL(**1b**$^-$ + MeOH). Based on HF and MP2 calculations, this difference in energy is 15.5 and 12.1 kcal/mol, respectively.

**TBP Intermediates.** Four minima were located for the TBP structures corresponding to $I^{TBP}_B$: the torsional isomers with regard to the exocyclic P−OMe bond ($I^{TBP}_{B(g)}$, $I^{TBP}_{B(t)}$, $I^{TBP}_{B(-g)}$) and an isomer with the nitrogen atom inverted ($I'^{TBP}B(g)$). HF and MP2 calculations suggested that the conformational isomer $I^{TBP}_{B(g)}$, which has a *gauche* methoxyl group relative to the endocyclic sulfur, was the most stable. In all of the structures for $I^{TBP}_B$, the lone pair of the equatorial nitrogen was located almost coplanar to the equatorial ligands. This geometric feature should give rise to optimal $\pi$-bonding hyperconjugative interaction of the nitrogen lone pair with the two other equatorial ligands.[9,11−14]

Meanwhile, neither $I^{TBP}_A$ nor $I^{TBP}_C$, in which the sulfur atom occupies an axial position, could be located on the HF potential energy surface: geometry optimizations resulted in cleavage of the endocyclic P−S bond to yield tetrahedral species.

**Transition States for Cleavage/Formation of the P−O and P−S Bonds in $I^{TBP}_{B(g)}$.** In the transition states for formation/cleavage of exocyclic and endocyclic P−O bonds ($TS^x_{P-O}$ and $TS^n_{P-O}$), the phosphorus atom showed geometric features halfway between the tetrahedral tetracoordinate and TBP pentacoordinate states. The intrinsic reaction coordinate calculations indicated that the transition state $TS^x_{P-O}$ was connected to $I^{TBP}_{B(g)}$ and IL(**1b** + MeO$^-$). Thus, these transition states can be considered saddle points on the reaction coordinate for the in-line process.

We located two transition-state structures for cleavage of the endocyclic equatorial P−S bond, in which the lone pair on the nitrogen atom is antiperiplanar and synperiplanar, respectively, relative to the exocyclic P−S bond. The former transition state $TS^n_{P-S}$ was slightly lower in energy than the latter $TS'^n_{P-S}$. The structures of the transition states $TS^n_{P-S}$ and $TS'^n_{P-S}$ are characterized more accurately as square pyramidal phosphorus rather than either TBP or tetrahedral phosphorus. The exocyclic sulfur atom occupies the apical position in the square pyramid. The structure with square pyramidal phosphorus is a transition state for pseudorotation. Importantly, the TBP species $I^{TBP}_A$, which is believed to be an intermediate resulting from pseudorotation (pathway A), did not represent a local energy minimum. Thus, the

(26) Reed, A. E.; Curtiss, L. A.; Weinhold, F. *Chem. Rev.* **1988**, *88*, 899−926.
(27) Reed, A. E.; Schleyer, P. v. R. *Inorg. Chem.* **1988**, *27*, 3969−3987.
(28) Dejaegere, A.; Karplus, M. *J. Am. Chem. Soc.* **1993**, *115*, 5316−5317.
(29) Dejaegere, A.; Liang, X.; Karplus, M. *J. Chem. Soc. Faraday Trans.* **1994**, *90*, 1763−1770.
(30) Wong, M. W.; Frisch, M. J.; Wiberg, K. B. *J. Am. Chem. Soc.* **1991**, *113*, 4776−4782.
(31) Wong, M. W.; Wiberg, K. B.; Frisch, M. J. *J. Am. Chem. Soc.* **1992**, *114*, 523−529.
(32) Wong, M. W.; Wiberg, K. B.; Frisch, M. J. *J. Am. Chem. Soc.* **1992**, *114*, 1645−1652.
(33) Cieplak, A. S.; Wiberg, K. B. *J. Am. Chem. Soc.* **1992**, *114*, 9226−9227.
(34) Wong, M. W.; Wiberg, K. B.; Frisch, M. J. *J. Comput. Chem.* **1995**, *16*, 385−394.
(35) CCDC, University Chemical Laboratory, Cambridge, U.K.
(36) The largest deviations in the endocyclic bond lengths and bond angles are 0.037 Å (S−C bond) and 6.1° (bond angle about P−O−C), respectively. The deviations in the exocyclic P−S and P−N bond lengths are less than 0.01 Å.

**Chart 1. Syn and Anti Regions of the Phosphate Moiety**

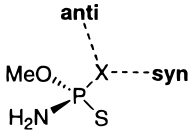


X = O: $TS^{elim\text{-}T}$, $Pdt_{A/C}$
X = S: $TS^{elim\text{-}O}$, $Pdt_B$

transition state $TS^{n}{}_{P-S}$ should be a saddle point not only for the pseudorotation in $I^{TBP}{}_B$ but also for cleavage of the equatorial P−S bond. The intrinsic reaction coordinate analysis indicated that the reaction coordinate for cleavage of the P−S bond was strongly coupled with that for pseudorotation in the TBP intermediate $I^{TBP}{}_B$.

**Tetrahedral Intermediates.** The tetrahedral intermediates and the subsequent stationary point structures that were considered for reaction pathway C are enantiomers of those for reaction path A. Therefore, we hereafter only consider the stationary points along pathways A and B.

Due to conformational freedom in the *β*-thioethyl or *β*-oxyethyl side chain, several rotational isomers are possible for tetrahedral intermediates. We used AM1 Hamiltonian for systematic conformational analysis and then performed HF geometry optimizations for rotational isomers with the lowest energy. In the optimized structures of $I^{TH}{}_A$ and $I^{TH}{}_B$, either the thio anion or the oxy anion at the terminus of the side chain was located close to one of the N−H protons. In addition, the thio or oxy anion was almost collinear to the N−H bond. These geometric features suggest favorable intramolecular electrostatic interactions between the negative charge at the terminus of the side chain and the N-H protons. Indeed, MP2 optimization starting from the HF geometry of $I^{TH}{}_B$ resulted in a hydrogen shift from the nitrogen atom to the oxygen atom at the terminus of the *β*-oxyethyl side chain.

**Transition States for the Elimination of Thiirane and Oxirane.** Elimination of thiirane or oxirane from the tetrahedral intermediates $I^{TH}{}_A$ and $I^{TH}{}_B$ occurs via an $S_N2$-type nucleophilic attack of thio/oxy anion at the carbon atom. We were able to locate four transition states for the elimination of thiirane (TS's$^{elim\text{-}T}$) and four other transition states for the elimination of oxirane (TS's$^{elim\text{-}O}$). The four transition states for each process were energetically comparable. Departing thiirane and oxirane moieties were located in either the syn or anti region of the resulting phosphoramidothioate $Pdt_A$ and phosphoramidodithioate $Pdt_B$ (Chart 1). Two transition states, which had different directions for the thiirane/oxirane moiety, were found for both syn and anti departure. It is noteworthy that the transition states TS's$^{elim\text{-}O}$ were significantly higher in energy than TS's$^{elim\text{-}T}$.

**Long-Range Complexes of the Products.** As for the reactants, long-range ion−dipole minima were found for the products. Thiirane and oxirane molecules were located in the syn region (see Chart 1) of phosphoramidothioate $Pdt_A$ and phosphoramidodithioate $Pdt_B$. The complex IL($Pdt_A$ + thiirane) resulting from pathway A is asymmetric ($C_1$). The molecular plane of thiirane was significantly tilted from the nonbridging O−P−S plane of $Pdt_A$. The nonbridging oxygen atom in $Pdt_A$ was

**Scheme 3. Reaction Pathways Suggested by ab Initio Calculations**[a]

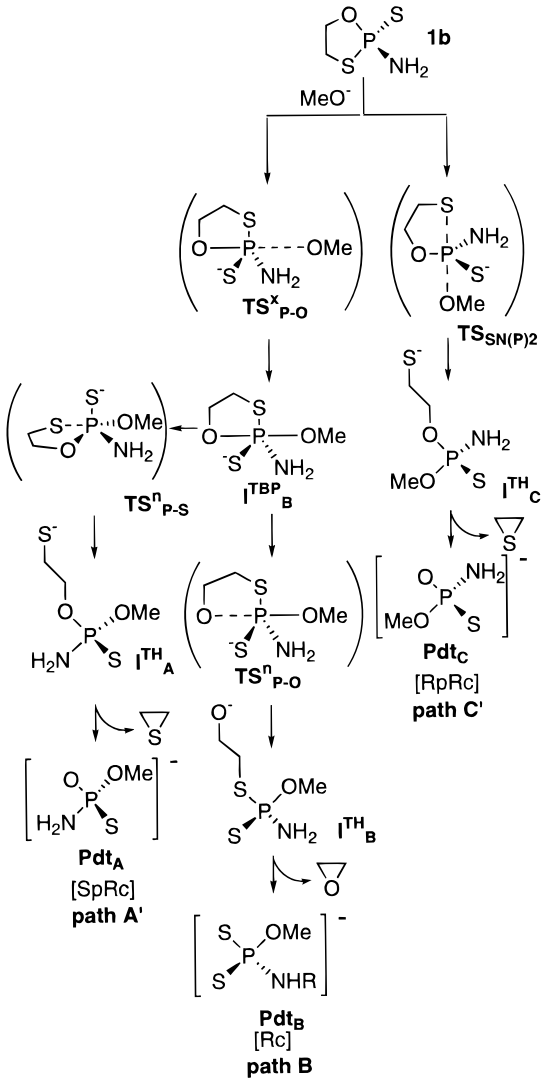


[a] The transition-state structures are shown in parentheses.

located closer to oxirane than the nonbridging sulfur atom. The ion−dipole minimum [IL($Pdt_B$ + oxirane)] resulting from pathway B has $C_s$ symmetry due to molecular symmetry. The oxirane molecule was located nearly coplanar to the S−P−S plane of $Pdt_B$. Rotating oxirane by 90° yields another $C_s$ structure, IL′($Pdt_B$ + oxirane), which was found to be a transition state with slightly higher energy.

**Conformation of the Products.** Thiirane and oxirane had only one structure with $C_{2v}$ symmetry. Phosphoramidothioate $Pdt_A$ had three distinct conformers, in which the methoxyl group adopted a *gauche*, *−gauche*, or *trans* conformation relative to the amino group ($Pdt1_A$, $Pdt2_A$, and $Pdt3_A$). The energies of these conformers were comparable. Meanwhile, phosphoramidodithioate $Pdt_B$ had a mirror plane in the global minimum ($C_s$ structure). Another $C_s$ structure was found to be a transition state ($Pdt'_B$).

**Transition-State Structure with a Ligand Arrangement Corresponding to $I^{TBP}{}_C$.** The TBP intermediate $I^{TBP}{}_C$, which has been postulated along reaction pathway C, could not be located on the potential energy surface. The TBP structure with a ligand arrangement corresponding to $I^{TBP}{}_C$ was possible merely as a saddle

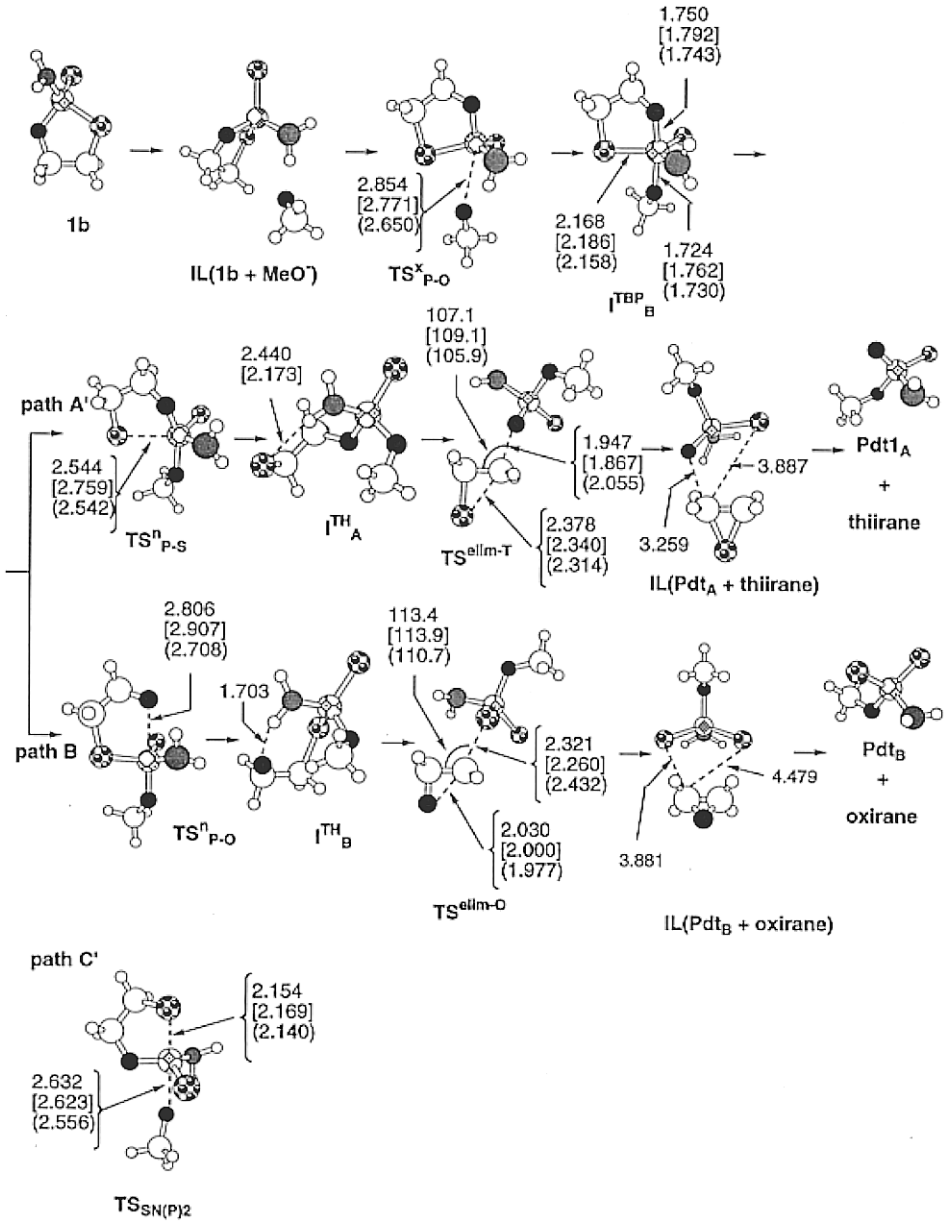


**Figure 1.** Structures of the stationary points along the lowest energy paths for reaction pathways A′, B, and C′. The gas-phase [HF and MP2 (in brackets)] and solution-phase (in parentheses) geometric parameters are given in Å and degrees.

point ($TS_{SN(P)2}$). A frequency calculation analysis suggested a one-step addition−elimination mechanism: nucleophilic attack of methoxide collinear to the endocyclic P−S bond should occur in concert with breaking of the P−S bond. The geometric features of $TS_{SN(P)2}$ indicated that the transition state had highly asynchronous character. The length of the forming exocyclic P−O bond in $TS_{SN(P)2}$ was significantly longer than that of the corresponding P−O bond in the most stable TBP intermediate $I^{TBP}_{B(g)}$ (2.623 vs 1.762 Å for the MP2 geometries). In contrast, the breaking P−S bond in the axial position was even shorter than the equatorial P−S bond in $I^{TBP}_{B(g)}$ (2.169 vs 2.186 Å).

**Solvation Effects.** We carried out HF geometry optimizations through the Onsager model for the six transition states $TS^{x}_{P-O}$, $TS^{n}_{P-O}$, $TS1^{elim-O}$, $TS^{n}_{P-S}$, $TS1^{elim-T}$, and $TS_{SN(P)2}$, as well as for the most stable TBP intermediate $I^{TBP}_{B(g)}$. The Onsager model did not significantly alter the gas-phase geometries. For the TBP intermediate $I^{TBP}_{B(g)}$, the differences between the gas-phase and solution-phase geometries were less than 0.01 Å and 1° for bond lengths and bond angles, respectively. Comparable differences were found for the transition states $TS^{n}_{P-S}$. Slightly larger differences were observed for other transition states.[37]

The Onsager model calculations provided an estimate of solvation energies for the stationary points. The transition states $TS^{x}_{P-O}$, $TS1^{elim-T}$, $TS1^{elim-O}$, and $TS_{SN(P)2}$ were found to be better solvated than the TBP intermediate $I^{TBP}_{B(g)}$. On the other hand, the solvation energies for the transition states $TS^{n}_{P-S}$ and $TS^{n}_{P-O}$ were comparable to that for the TBP intermediate $I^{TBP}_{B(g)}$ and were relatively small (see Figure 3).

(37) For the transition states $TS^{x}_{P-O}$ and $TS^{n}_{P-O}$, the breaking/forming P−O bonds were shortened by 0.204 and 0.098 Å, respectively, in the solution phase compared with those in the gas phase. Similarly, the forming P−O bond and the breaking P−S bond in $TS_{SN(P)2}$ were shortened by 0.076 and 0.014 Å, respectively. Meanwhile, the Onsager model suggested transition states $TS1^{elim-T}$ and $TS1^{elim-O}$, with breaking O−C and S−C bonds 0.108 and 0.111 Å longer than the corresponding gas-phase geometries. Conversely, the forming C−S and C−O bonds are 0.064 and 0.053 Å shorter in the solution phase.

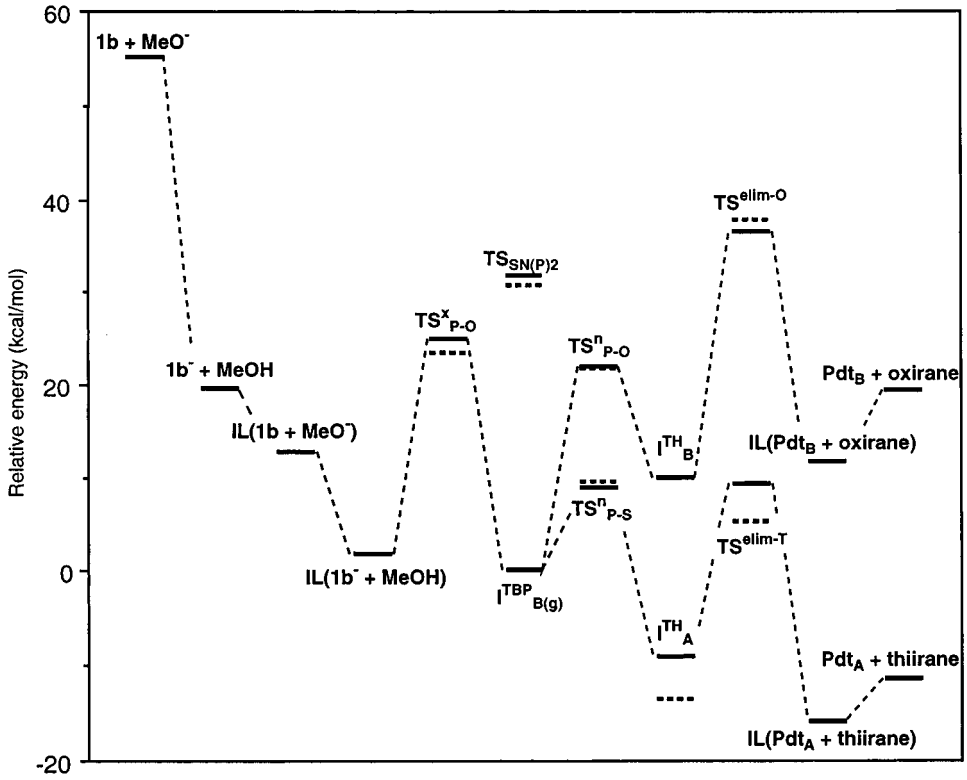


**Figure 2.** Gas-phase profiles of the potential energy surface. The energies of each stationary point relative to the TBP intermediate $I^{TBP}_{B(g)}$ are shown: (a) solid lines, calculated at the level of MP2/6-31+G*//HF/6-31+G* [corrected for zero-point energies (scaled by a factor of 0.8929) calculated at the HF level] and (b) broken lines, calculated at the level of MP4(DQ)/6-31+G*//MP2/6-31+G* (corrected for zero-point energies calculated at the MP2 level).

## Discussion

Our results point to the three reaction pathways summarized in Scheme 3. These pathways correspond to pathways A−C in Scheme 1. Figure 1 shows the optimized structures of the stationary points along each pathway. First, the collinear attack of methoxide will occur from the side opposite the endocyclic P−O bond, resulting in the TBP intermediate $I^{TBP}_B$ through the transition state $TS^x_{P-O}$. Pseudorotation in $I^{TBP}_B$ will occur concomitant with cleavage of the endocyclic P−S bond via the transition state $TS^n_{P-S}$ to immediately give the tetrahedral intermediate $I^{TH}_A$, without forming $I^{TBP}_A$ (pathway A′ in Scheme 3; indicated by the broken arrow in Scheme 1). No TBP minimum with a ligand arrangement of $I^{TBP}_A$ was located on the potential energy surface. Concerted pseudorotation and cleavage of the equatorial P−S bond in the TBP intermediate $I^{TBP}_B$ is noteworthy. A similar addition−elimination mechanism along with pseudorotation was originally suggested by Lim and Tole for hydrolysis of neutral methyl ethylene phosphate.[15,16] Second, collapse of the TBP intermediate $I^{TB}_B$ in the in-line mechanism may result in the tetrahedral intermediate $I^{TH}_B$ (pathway B). Finally, attack of methoxide collinear to the endocyclic P−S bond may cause immediate ring opening of 1,3,2-oxathiaphospholane to yield the tetrahedral intermediate $I^{TH}_C$ via the transition state $TS_{SN(P)2}$ (pathway C′, Scheme 3). Elimination of thiirane or oxirane will convert the tetrahedral intermediate $I^{TH}_A$, $I^{TH}_B$, or $I^{TH}_C$ to phosphoramidothioate $Pdt_A$ or $Pdt_C$ or phosphoramidodithioate $Pdt_B$.

Not only in the gas phase but also in the solution phase, pathway A′ will be preferred over either pathway B or C′ (Figures 2 and 3). In our highest level calculations (MP4(DQ)), the relative energies of the stationary points appear to converge in this respect (Table 1). The transition state ($TS_{SN(P)2}$ along pathway C′) for the attack of methoxide collinear to the endocyclic P−S bond was 7.2 kcal/mol higher in MP4 energy than that for collinear attack from the side opposite the endocyclic P−O bond ($TS^x_{P-O}$). The transition states $TS^n_{P-O}$ and $TS^{elim-O}$ along pathway B were higher in energy by 12.2 and 32.4 kcal/mol, respectively, than the corresponding transition states along pathway A′ ($TS^n_{P-S}$ and $TS^{elim-T}$). Thus, pathway A′ for the addition−elimination mechanism concerted with pseudorotation followed by elimination of thiirane is most likely for the nucleophilic ring opening of 1,3,2-oxathiaphospholane. This mechanism is consistent with the experimentally determined chemo- and stereoselectivity. The preference for the TBP ligand arrangement of $I^{TBP}_B$ over those of $I^{TBP}_A$ and $I^{TBP}_C$ is consistent with the general guidelines of apicophilicity.[9,11−14] A bulky substituent prefers an equatorial position.[5] Since the compound used for this experiment (**1a**) had a large α-naphthylethyl group on the nitrogen atom, the TBP ligand arrangement of $I^{TBP}_A$, with the nitrogen ligand in an axial position, should be highly improbable for the actual system.

The significant energy difference between pathways A′/C′ and B can be interpreted as arising from the difference in polarizability and electronegativity between oxygen and sulfur atom. Since the oxygen atom is less polarizable than the sulfur atom, oxy anion is disfavored over corresponding sulfur anion. Thus, the tetrahedral intermediate $I^{TH}_B$, with a negative charge on the oxygen atom at the terminus of the chain, is much higher in energy than the corresponding intermediate $I^{TH}_A$ with a negative charge on the sulfur atom at the same location. The energy difference between $I^{TH}_A$ and $I^{TH}_B$ (HF, 33.1;

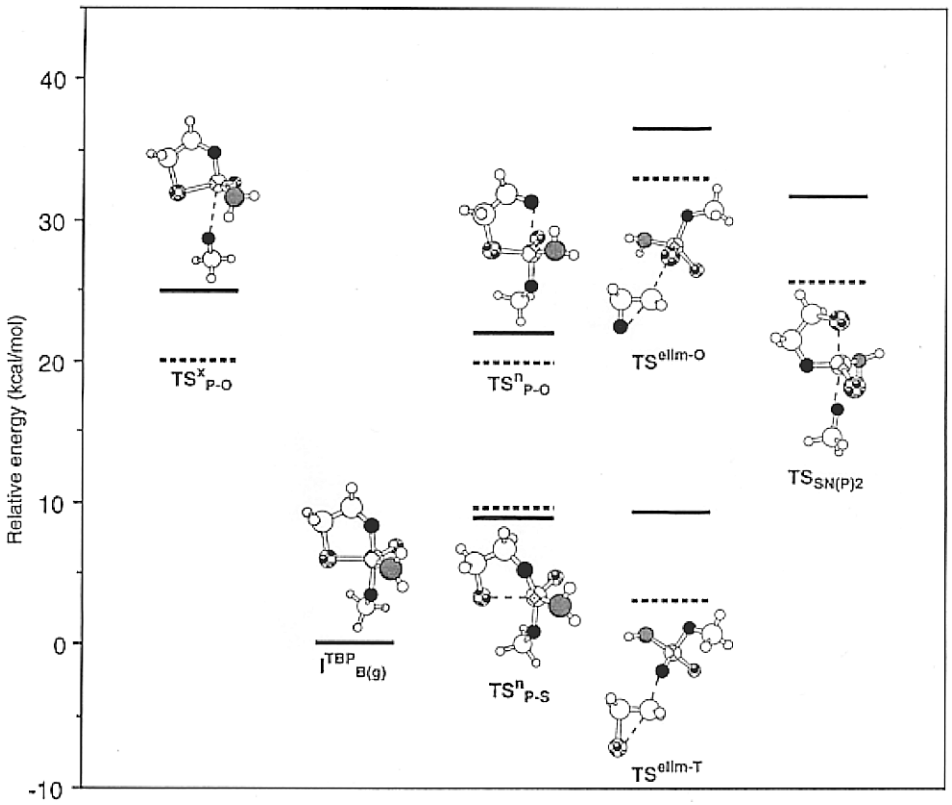


**Figure 3.** Gas-phase and solution-phase (broken lines) potential energies of the transition states relative to the TBP intermediate $I^{TBP}_{B(g)}$. The energies were evaluated at the MP2 level at the HF geometries [corrected for zero-point energies (scaled by a factor of 0.8929) calculated at the HF level].

**Table 1. Relative Energies of the Stationary Points (in kcal/mol)**

| | //HF/6-31+G* [a] | | //MP2/6-31+G* [b] | |
|---|---|---|---|---|
| structure | $E_{HF}$ | $E_{MP2}$ | $E_{MP2}$ | $E_{MP4(DQ)}$ |
| $TS^{x}_{P-O}$ | 21.23 | 24.88 | 23.25 | 23.48 |
| $I^{TBP}_{B(g)}$ | 0.00 | 0.00 | 0.00 | 0.00 |
| $TS^{n}_{P-S}$ | 7.35 | 8.84 | 9.65 | 9.41 |
| $TS^{elim-T}$ | -8.27 | 9.27 | 6.28 | 5.28 |
| $TS^{n}_{P-O}$ | 17.67 | 22.01 | 22.23 | 21.64 |
| $TS^{elim-O}$ | 29.42 | 36.53 | 35.80 | 37.69 |
| $TS_{SN(P)2}$ | 27.77 | 31.75 | 30.34 | 30.70 |

[a] Corrected for zero-point energies calculated at the HF level (scaled by a factor of 0.8929). [b] Corrected for zero-point energies calculated at the MP2 level.

MP2, 20.2 kcal/mol) is significantly reduced when one of the protons on the nitrogen atom has been transferred to the terminal oxygen or sulfur atom ($I'^{TH}_{A}$ and $I'^{TH}_{B}$; HF, 5.5; MP2, 8.8 kcal/mol).

In addition, the magnitude of hyperconjugative stabilization in the tetrahedral phosphorus component changes significantly when the P−O bond is replaced with the P−S bond. The P−O bond is shorter than the P−S bond. Moreover, since oxygen is more electronegative than sulfur, the P−O bond has a higher ionic character than the P−S bond. The lobe on the outer face of the phosphorus atom is larger for the P−O antibond than for its P−S counterpart. As a consequence, the oxygen lone pairs and the P−O antibond have greater overlap with other unfilled antibonding and filled bonding orbitals, respectively, compared with the sulfur lone pairs and the P−S antibond. Thus, hyperconjugative stabilization is considerably greater for the P−O component than for the P−S component. The magnitude of this hyperconjugative stabilization can be evaluated by deleting the off-diagonal Fock matrix elements in the NBO basis. The stabilization energies due to hyperconjugation associated with the lone pairs on the oxygen/sulfur atom and the P−O/P−S antibond in the P−$XCH_2$ component were calculated to be 137 and 86 kcal/mol, respectively, for $I^{TH}_{A}$ (X = O) and $I^{TH}_{B}$ (X = S). The same trend was observed for hyperconjugative stabilization associated with the P−O and P−S components in the final products $Pdt_A$ and $Pdt_B$ (185 and 111 kcal/mol, respectively).

## Conclusions

We carried out theoretical investigations on the mechanism of base-catalyzed methanolysis of 1,3,2-oxathiaphospholane (eq 1). Our gas-phase ab initio calculations suggested that reaction pathway A′ (Scheme 3) should be the most energetically favorable among the possible pathways shown in Scheme 1. The TBP intermediate $I^{TBP}_{B}$, which results from nucleophilic attack of methoxide anion at the phosphorus atom, will undergo concerted pseudorotation and cleavage of the endocyclic P−S bond to immediately give the tetrahedral intermediate $I^{TH}_{A}$. No local minimum was found on the potential energy surface for the TBP structure $I^{TBP}_{A}$, which is expected from the pseudorotation of $I^{TBP}_{B}$. Onsager model calculations suggested that the gas-phase reaction profiles should not be altered intrinsically in the solution phase (Figure 3). Thus, reaction pathway A′, in which addition−elimination in concert with pseudorotation is followed by elimination of thiirane, is the most likely mechanism for the nucleophilic ring opening of 1,3,2-oxathiaphospholane. This mechanism enables us to interpret the experimentally determined chemo- and stereoselectivity for the ring opening of 1,3,2-oxathiaphospholane.

Lim and Tole first reported that addition−elimination in concert with pseudorotation was a viable reaction coordinate for substitution with a retention of configuration at a phosphorus atom.[15,16] A concerted pseudorotation mechanism has been reported for other related systems.[17,18] Our results extend their mechanism to nucleophilic ring opening in the 1,3,2-oxathiaphospholane system. Thus, even though the TBP species resulting from pseudorotation is significantly unstable compared with the original TBP intermediate and fails to exist as an intermediate, substitution can occur with a retention of configuration at phosphorus. In such cases, pseudorotation will occur in concert with substitution: bending of the bonds of both the axial and equatorial ligands in the TBP species should be coupled with the reaction coordinate for the substitution. Indeed, if pseudorotation causes replacement of the original apicophilic axial ligands with others that are less apicophilic, then the new TBP will fail to represent a local energy minimum.[14,38,39] The findings described here provide interesting implications for the chemistry of phosphoranes, especially with regard to the mechanism of the hydrolysis of phosphates and related derivatives.

**Acknowledgment.** The services and computational time made available by the Research Information Processing Center (RIPS) have been essential to this study and are gratefully acknowledged. T.U. thanks Drs. Shuitiro Ono (Director General of the National Institute of Materials and Chemical Research), Kazutoshi Tanabe, Seiji Tsuzuki, and Takuji Hirose for their encouragement and helpful discussions.

**Supporting Information Available:** Tables of (i) the absolute energies (Supplementary Tables 1−3) and (ii) the optimized geometric parameters (Supplementary Tables 4−12), figures showing the optimized stationary point structures, including those not shown in Figure 1 (Supplementary Figures 1−9), and Cartesian coordinates of the stationary point structures optimized at the MP2 level (29 pages). This material is contained in libraries on microfilm, immediately follows this article in the microfilm version of the journal, and can be ordered from the ACS; see any current masthead page for ordering information.

JO962220U

(38) Wang, P.; Agrafiotis, D. K.; Streitwieser, A.; Schleyer, P. v. R. *J. Chem. Soc., Chem. Commun.* **1990**, 201−203.
(39) Wasada, H.; Horao, K. *J. Am. Chem. Soc.* **1992**, *114*, 16−27.